Effects of internal stress on remanence intensity jumps across the Verwey transition for multi-domain magnetite

Qingsong Liu[1,2*], Yongjae Yu[3], Adrian R. Muxworthy[4], Andrew P. Roberts[2]

1. Paleomagnetism and Geochronology Laboratory (SKL-LE), Institute of Geology and Geophysics, Chinese Academy of Sciences, Beijing 100029, Peoples' Republic of China.

2. National Oceanography Centre, University of Southampton, European Way, Southampton SO14 3ZH, United Kingdom

3. Department of Geology and Earth Environmental Sciences, Chungnam National University, Daejeon, 305-764, Korea

4. Department of Earth Science and Engineering, Imperial College London, South Kensington Campus, London SW7 2AZ, United Kingdom.

* Corresponding author: Qingsong Liu, liux0272@yahoo.com

Abstract

The magnetic properties of magnetite (Fe_3O_4) are strongly dependent on the internal stress related to stressed-controlled regions and to closure domains associated with defects. The contribution of internal stress to the low-temperature magnetic properties of magnetite was tested using annealed and unannealed multi-domain (MD) magnetites. During low-temperature cooling, a room-temperature-induced saturation isothermal remanent magnetization (SIRM) increased abruptly at the Verwey transition (T_v ~122 K). In particular, the absolute intensity jump (δ_{VJ}, defined as the jump in SIRM at T_v upon cooling) resulted from the high-coercivity fraction of MD grains. We observe that annealing significantly reduces internal stress and thus decreases the average microcoercivity. Comparison of the alternating field (AF) demagnetization spectra of δ_{VJ} both for annealed and unannealed magnetites directly links δ_{VJ} to the internal stress. It is likely that removal of the closure domain associated with stress-controlled regions was dominant when the peak AF was less than the average micromagnetic coercivity $<h_c>$, resulting in a net increase of δ_{VJ} with increasing AF. However, when the AF exceeded the $<h_c>$ threshold, δ_{VJ} decreased because the stress-controlled regions were demagnetized. Such observations could therefore be useful for estimating the $<h_c>$ of MD magnetite.

Key words: Verwey transition, magnetite, internal stress, AF demagnetization, closure domain.

1. Introduction

Low-temperature magnetic measurements have become increasingly popular in environmental magnetism and paleomagnetism as a means of non-destructively identifying magnetic minerals, many of which display magnetic anomalies associated with various types of physical transitions. For instance, the Verwey transition (~122 K, T_v) indicates the presence of magnetite (Fe_3O_4) in rocks, sediments, and soils (Nagata et al., 1964; Ozima et al., 1964a, 1964b). At the Verwey transition, many magnetic, electronic and crystallographic properties of magnetite change. In particular, the crystallographic cubic symmetry changes to (arguably) monoclinic symmetry. This change in symmetry strongly affects the magnetocrystalline anisotropy of magnetite, which is an order of magnitude larger in the monoclinic phase than in the cubic phase (Kakol et al., 1992, 1994; Muxworthy & McClelland, 2000a). In addition to the Verwey transition, the cubic magnetocrystalline anisotropy of magnetite has an isotropic point T_i at 130 K, which also influences its low-temperature magnetic behaviour (Muxworthy & McClelland, 2000a; Özdemir et al., 2002).

In multi-domain (MD) magnetite, these large variations in anisotropy directly influence various magnetic properties. For example, upon cooling through T_v the coercive force increases and the susceptibility decreases (Muxworthy & Williams, 1999; Özdemir et al., 2002). Similarly, the change in sign and magnitude of anisotropy constants causes demagnetization of a saturation isothermal remanent magnetization (SIRM) induced in MD magnetite on either heating or cooling through T_v (Özdemir & Dunlop, 1999). The mechanisms controlling low-temperature demagnetization during low-temperature cycling (LTC) are still debated.

Magnetic coercivity in MD magnetite is the sum of the flipping moment of magnetization as a result of domain pinning and/or wall nucleation, where internal stress controls domain wall pinning and nucleation (Xu and Merrill, 1989, 1992). Magnetic coercivity reflects such domain creation/reorganization in response to variation of external fields. One powerful tool in deciphering the origin of magnetic coercivity is the temperature dependence of magnetic hysteresis (e.g., Dunlop, 1987; Smirnov and Tarduno, 2002; Yu et al., 2004). For example, temperature dependence of coercivity at high temperatures (300-870 K) indicates that crystal defects of magnetoelastic origin control the coercivity (Hodych, 1982, 1990; Özdemir and Dunlop, 1997). This interpretation needs modification at 300-170 K, where coercivity is mainly controlled by magnetostriction (Özdemir, 2000). Below 170 K, Özdemir (2000) documented that coercivity depends on magnetostriction as well as magnetocrystalline anisotropy. In addition to temperature dependent approaches, addition/removal of static pressure also reveals that internal stress is a key factor that governs the magnetic properties of magnetite (e.g., Gilder et al., 2004, 2006).

In general, upon cooling from 300 K to slightly above T_v, remanences carried by MD grains are found to gradually decrease. This irreversible demagnetization is due to the reduction in magnetocrystalline anisotropy. Upon passing through T_v, thermomagnetic curves commonly change abruptly, although detailed remanence variation is strongly dependent on the type of initial room temperature magnetization. SIRM appears either to stop demagnetizing on reaching T_v, and undergoes little or no variation with temperature below T_v, or a small proportion of remanence associated with the high-coercivity fraction displays abrupt increases or "jumps" at T_v that are partially reversible upon warming

(Muxworthy & McClelland, 2000b; Özdemir et al., 2002; Muxworthy et al., 2003; Yu et al., 2003a). For example, for fine-grained magnetites, the SIRM cooling curve changed little with temperature (Yu et al., 2003a). In contrast, for the 1.3 mm single crystal, the remanence decreased much more than for other samples and in addition, a jump in intensity occurred when passing through T_v (Özdemir et al., 2002). As in earlier studies, the magnitude of the jump at T_v is hereafter referred to as δ_{VJ}. Muxworthy et al. (2003) defined a similar parameter Δ_{VJ} as the absolute jump in intensity divided by the intensity of the initial remanence at 300 K. In the present study, δ_{VJ} is used to define the absolute intensity jump in crossing T_v. It is worth noting that δ_{VJ} was recognized by examining partial thermoremanent magnetizations and the anhysteretic remanent magnetization (ARM) or by partially demagnetizing SIRMs (Muxworthy & McClelland, 2000b; Muxworthy et al., 2003). To further investigate the origin of δ_{VJ} at T_v, we have studied the low-temperature magnetic behaviour for a set of MD magnetites with and without annealing, to better understand the effects of internal stress on δ_{VJ}.

2. Samples and experiments

MD magnetites with two different origins were studied: synthetic polycrystalline magnetite produced by Wright Industries, and a natural magnetite crushed from a massive magnetite block collected from the Central African Republic and provided by IKON Mining Company. The synthetic samples are labeled W041183 and W112982 with a nominal manufacturer's grain size of ~15-20 μm and ~40 μm, respectively. Various grain sizes have been reported for these two commercial magnetites (W041183 and W112982): 40 and 37.4 μm (Jackson et al., 1990); 18 ± 12 and 17 ± 8 μm (Yu et al.,

2002). Magnetic hysteresis data for both samples at room temperatures are similar. For W112982, the ratio of the saturation remanent magnetization (M_{rs}) to the saturation magnetization (M_s) is $M_{rs}/M_s = 0.057$, and the ratio of the remanence coercivity (B_{cr}) to the coercivity (B_c) is $B_{cr}/B_c = 6.468$. For sample W041183, $M_{rs}/M_s = 0.065$, and $B_{cr}/B_c = 5.137$ (Yu et al., 2002). Both samples fall in the MD range according to the criteria of Day et al. (1977). The natural sample is not a single crystal; it is a fragment that was removed from a large block. It has an elongated shape with approximate dimensions of ~4 mm in length and ~2.5 mm in diameter.

Low-temperature oxidation is a common phenomenon and can change the magnetic properties of MD magnetite. Surficial stress, associated with low-temperature oxidation, and internal stress can both be reduced by annealing. To effectively reduce internal dislocations, annealing requires heating up to 700-800°C for a few hours (e.g., Dunlop and Özdemir, 1997). The movement of dislocations is similar to what is variously termed in rheology as dislocation, power-law, high-temperature or Weertman creep (Weertman, 1978; Putnis, 1992). This type of creep increases with temperature ($\propto e^{t/t_M}$) and becomes significant in the range 0.3-0.7 t/t_M, where t is the temperature and t_M the melting temperature (t_M ~1534°C for magnetite). Dislocation creep is commonly removed from samples by "thermal stabilization" (e.g., Sholpo et al., 1991).

To anneal these MD magnetites, temperature-dependence of magnetic susceptibility (χ-T) was measured up to 700°C (Fig. 1) with heating in an argon atmosphere. The samples were held for 2 hours at 700°C. All of the samples shown in Figure 1a-c were subjected to a second heating-cooling cycle (Figure 1d-f). Even in this second heating-cooling cycle, a decrease in susceptibility due to surficial oxidation is still observed for

sample W041183 (Figure 1d). On the other hand, the second heating-cooling cycle results in nearly reversible thermomagnetic curves for W112982 (Figure 1e) and for the mm-size magnetite (Figure 1f). After complete heating/cooling cycles, the samples generally have slightly lower susceptibilities. For the two powdered samples, there are two possible mechanisms to explain these reductions. These two magnetite samples have been stored in air for many years, therefore it is likely that they have rims of surficial maghemite due to low-T oxidation. In terms of volume percentage, the effect of such oxidation would be greater for smaller grains for the same degree of oxidation. Upon heating, this maghemite rim will convert to hematite at about 350°C. However, associated with oxidation rims are stresses due to mismatches in lattice spacings. We expect that annealing will effectively reduce the surficial stress by converting the surface rims to hematite, which will reduce stress between the interior and rim of the grain. The net effect of the annealing is still a reduction of internal stress, which is what we aim to address in this study.

Low-temperature experiments were conducted using a Quantum Designs Magnetic Properties Measurement System (MPMS) before and after the annealing experiments described above. The ambient field inside the MPMS was reduced to < ~50 μT. Such a weak internal field has insignificant effects on LTC of SIRM. To thermally demagnetize a low-temperature SIRM, the samples were first cooled to 10 K, an SIRM was imparted in a field of 2.5 T, and the SIRM was then measured during warming to 300 K. LTC measurements were performed for a 2.5 T SIRM induced at room-temperature after alternating field (AF) demagnetization of both fresh and annealed samples. This residual remanence is denoted as $SIRM_{x\,mT}$, where x mT is the peak AF. For example, $SIRM_{15\,mT}$ represents a residual remanence after AF demagnetization of the SIRM at a peak AF of

15 mT. ARM was also imparted in a 200 mT AF with a superimposed 50 μT direct bias field using a DTECH D2000 instrument. Upon completion of low-temperature experiments, temperature dependence of magnetic hysteresis was measured both for unannealed and annealed samples from room temperature to 575°C at 25°C steps to check whether the influence of internal stress on low-temperature magnetic properties is evident at high temperatures.

3. Results

Values of B_c for all three measured samples systematically decrease after annealing: from 7.67 to 5.16 mT for W041183 (15-20 μm), from 2.30 to 1.98 mT for W112982 (40 μm), and from 0.92 to 0.78 mT for the mm-size magnetite, respectively (Fig. 2). For MD magnetite, the bulk coercivity is mainly controlled by the distribution of internal stress (Xu & Dunlop, 1995). Therefore, a systematic decrease in B_c after annealing strongly indicates efficient elimination of internal stress.

Temperature-dependence of magnetic coercivity at high temperatures is evident for both unannealed and annealed samples. With increasing temperature, coercivity decreases. The coercivity for the unannealed ("raw") samples decays faster than for the annealed samples below 425°C (Fig. 3).

Thermal demagnetization results for a low-temperature SIRM (LTSIRM, which is defined as a 2.5 T SIRM imparted at 10 K) (Fig. 4a-c) indicate that the LTSIRM decreases sharply on warming through T_v. LTC curves for a room temperature SIRM (a 2.5 T SIRM acquired at 300 K) have a smaller intensity jump during cooling through ~120-130 K (Fig. 4d-f). When subjecting the SIRM to AF demagnetization at fields <60-

70 mT, δ_{VJ} has only a small amplitude regardless of demagnetization level (Fig. 5), although the initial SIRM is substantially demagnetized. This indicates that the processes controlling δ_{VJ} are not directly dependent on the initial remanence for the mm-size magnetite. For W041183 (15-20 μm), there are great differences in LTC behaviour. The most notable feature is that δ_{VJ} is suppressed for the annealed sample (Fig. 6). A detectable jump occurs only when the AF exceeds 30 mT.

The AF demagnetization spectra of δ_{VJ} for unannealed samples are strongly grain-size dependent (Fig. 7). With increasing grain size, initial δ_{VJ} values are gradually enhanced and the peak δ_{VJ} gradually shifts to higher AF values. After annealing, the AF dependency of δ_{VJ} is fundamentally changed. For example, δ_{VJ} for the annealed W041183 (15-20 μm) is significantly reduced, and is masked by the background remanence. Therefore, no reliable AF demagnetization spectrum of δ_{VJ} could be constructed for this sample. For W112982 (~40 μm), the peak δ_{VJ} at 30 mT for the raw sample disappears upon annealing, and δ_{VJ} consistently decreases with increasing AF (Fig. 7). After annealing, the mm-size magnetite has decreasing δ_{VJ} with increasing AF, but with a broader peak centered at around 70 mT before δ_{VJ} decreases to zero (Fig. 7).

AF demagnetization spectra of ARM and SIRM and the corresponding ratio of ARM to IRM for the mm-size magnetite are illustrated in Fig. 8. Unlike the δ_{VJ} spectra (Fig. 7), ARM and SIRM are almost completely demagnetized at 60 mT (Fig. 8a). The ARM/SIRM ratio is also AF dependent. With increasing AF, the ARM/SIRM ratio gradually increases (Fig. 8b).

4. Discussion

Muxworthy et al. (2003) demonstrated that δ_{VJ} is associated with the high-coercivity (or magnetically hard) fraction of MD grains, which was commonly thought to be controlled by internal stress due to defects and dislocations in the crystal lattice. Our results confirm their proposition. The magnetization of pseudo-single domain (PSD) and MD magnetite includes contributions from both high- and low-coercivity (or soft) fractions (e.g., Roberts et al., 2000; Dunlop et al., 2004). During AF demagnetization, the soft part of the SIRM can be easily demagnetized, but the hard fraction remains relatively stable, and can be destroyed only at elevated AF values. Thus, AF demagnetization is an efficient tool to discriminate between the magnetically hard and soft fractions. The SIRM of the mm-size magnetite is sufficiently demagnetized at 60 mT (Fig. 8a), while δ_{VJ} remains relatively stable at this high AF (Fig. 7a). This strongly indicates that δ_{VJ} is largely irrelevant to the soft fractions. Instead, it is controlled solely by the hard fractions that are much more resistant to AF demagnetization.

The Lowrie-Fuller test (Lowrie & Fuller, 1971) is a useful tool for determining the domain state of a magnetic remanence. Typically, the ARM carried by single-domain (SD) particles is more resistant to AF demagnetization than the corresponding SIRM, thus yielding ARM/SIRM > 1. For coarser-grained magnetites, an opposite pattern (ARM/SIRM < 1) has been observed, where ARM is much softer than the SIRM upon AF demagnetization (e.g., Yu et al., 2003b). Xu & Dunlop (1995) introduced an analytical model to explain the grain size-dependence of the Lowrie-Fuller test. They concluded that this apparent grain size-dependence is controlled by the internal stress distribution, which is, in turn, generally related to grain size. Therefore, when

ARM/SIRM > 1, remanence is controlled by higher internal stress. Our results demonstrate that ARM/SIRM is > 1 after AF demagnetization to 20 mT (Fig. 8b), which indicates that the magnetic coercivity is controlled by the magnetically hard fraction.

The hard fraction of the MD magnetization is generally associated with crystal defects such as inclusions, dislocations, grain boundaries and chemically altered regions, where closure domains are more easily formed (Özdemir & Dunlop, 1995). The strength of domain wall pinning is quantified by the microscopic coercivity h_c. For MD magnetite, there is a distribution of h_c values within grains, especially for natural samples. However, the magnetic complexity of MD grains is such that the distribution of these defects (or h_c) varies from sample to sample. This distribution is, in turn, determined by both the grain size of magnetic particles and the dislocation density (Xu & Dunlop, 1995).

Internal stress could also result from low-temperature oxidation, through which a thin maghemite rim could develop around a stoichiometric magnetite core. Internal stress is enhanced by the difference in lattice constant between the magnetite core and the maghemite rim (van Velzen & Zijderveld, 1992, 1995; Cui et al., 1994; van Velzen & Dekkers, 1999). Annealing can convert thermally unstable maghemite rims into weakly magnetic hematite, which is indicated by decreased magnetic susceptibility at ~350°C for the χ-T cooling curves (Fig. 1a, b). Thus, annealing can significantly reduce internal stress caused both by dislocations and by maghemite rims, and would decrease the magnetic stability. The distinct AF demagnetization spectra of δ_{VJ} before and after annealing strongly suggests that internal stress plays a key role in determining δ_{VJ}. Before annealing, δ_{VJ} is grain size dependent and the maximum δ_{VJ} value occurs at higher AF

values with increasing grain size. After annealing, systematic changes in δ_{VJ} disappear. Below is a tentative explanation for this magnetic behaviour.

For our samples, it appears that the microcoercivity distribution is grain size-dependent; therefore, the strong grain size-dependence of δ_{VJ} could be due to differences in the distribution of h_c. SD-like behaviour is associated with higher h_c. For a high-field remanence, such as SIRM, domain walls are likely be pushed beyond many strong pinning sites. Several workers have calculated the relationship between h_c and the macrocoercivity (e.g., Träuble, 1966; Xu & Merrill 1992). It has been shown that if a domain wall is pinned by a general stress field, the average h_c (= $<h_c>$) is a function of domain wall thickness. The $<h_c>$ reaches a maximum value when the wavelength of the stress field is about 5 times the wall thickness. If the domain wall is pinned by dislocations, larger MD samples will generally have a Gaussian coercivity distribution (Xu & Dunlop, 1995). Therefore, AF demagnetization spectra of δ_{VJ} could reflect the distribution of h_c. For example, the mm-size magnetite sample might therefore have a dominant $<h_c>$ of ~65 mT. For the 40 μm and 15-20 μm magnetite samples, the dominant $<h_c>$ values are reduced to about 30 and 10 mT, respectively (Fig. 7a). For the mm-size magnetite, the body domain can freely move at lower fields during AF demagnetization, while the closure domain near the strongly pinned parts can only undergo minor changes. Only above a threshold (e.g., ~65 mT) will the AF be high enough to overcome the microcoercivity of the pinned area, and demagnetization of the pinned parts occurs.

Contrary to unannealed samples, the annealed samples have magnetic characteristics that are somewhat similar to those of the hydrothermally produced sample H (108 μm) that is characterized by low internal stress (Muxworthy et al., 2003). For W041183 (15-

20 μm), the internal stress appears to have been significantly reduced by annealing as no intensity jump across T_v can be observed after annealing. The effect of AF demagnetization on the parameter δ_{VJ} for the mm-size magnetite sample is that it becomes magnetically "softer" after annealing. For example, prior to annealing, the parameter δ_{VJ} remains independent of AF demagnetization fields up to 60 mT. In contrast, after annealing, δ_{VJ} decays with increasing peak AF. This further reinforces the idea that internal stress controls the intensity jump across T_v.

We suggest two possible mechanisms to explain the intensity jump at T_v. The first mechanism involves the reduction in flowering for large SD-like structures. On the basis of micromagnetic simulations, the magnetic spins for SD particles have three different states (e.g., Schabes and Bertram, 1988; Williams and Dunlop, 1989). For the authentic SD state, magnetic spins are parallel with one another. In contrast, for a flower state, magnetic spins near the edge or corners of a grain slightly spread out. Thus, the flower state is one that is a little less uniformly magnetized. A vortex is a non-uniformly magnetized state with magnetic spins that curl with respect to the grain centre. However, such effects seem insignificant in our large MD grains. Second, it has been suggested that positive δ_{VJ} values may be caused by removal of closure-like domains (Muxworthy & Williams, 1999; Muxworthy & McClelland, 2000b; Özdemir et al., 2002; Muxworthy et al., 2003). Muxworthy & Williams (1999) demonstrated that upon cooling above T_v, the domain structure remains relatively stable, but that the large closure domains are significantly reduced when cooling through T_v, which results in the large δ_{VJ}. The AF demagnetization spectra of δ_{VJ} are, therefore, likely to be controlled by competition between an increase in intensity due to removal of closure domains and the decreased

intensity associated with the hard fraction due to AF demagnetization. That is, softer closure-domain-like features shield the harder fraction of the remanence, because when they are demagnetized in low AFs, δ_{VJ} increases. As the hard fraction is gradually demagnetized at higher AFs, δ_{VJ} will decrease. Based on this model, for the mm-size magnetite, the stable Δ_{VJ} below about 65 mT could indicate that the sample has high h_c. The stress-related domain wall pinning and the associated closure domains could be tightly pinned and therefore resistant to AF demagnetization. For such a case, δ_{VJ} will remain relatively stable when the peak AF is less than the upper limits of h_c. Above that, the hard fraction of remanence will be significantly reduced, resulting in a correspondingly large decrease in δ_{VJ}.

5. Conclusions

Our experimental results from unannealed and annealed MD magnetite samples lead to the following conclusions.

(1) For unannealed magnetites where stress is an important controlling factor on magnetic properties, δ_{VJ} is dependent on the grain size of magnetite.

(2) For annealed magnetites, the effects of AF demagnetization on δ_{VJ} are different from those before annealing. Results after annealing resemble the magnetic behaviour of large stress-free magnetite grains.

(3) The intensity jump across the Verwey transition during cooling from room temperature is controlled by stress-dominated regions within the MD magnetite grains.

(4) The impact of AF demagnetization on δ_{VJ} is controlled by two competing processes: an increase of the overall magnetization intensity by removal of closure domains associated with low-stress regions and decreased δ_{VJ} due to AF demagnetization

of the remanence carried by SD-like regions. While the SIRM is largely dominated by magnetically soft fractions, large δ_{VJ} is associated with stress-determined regions within MD magnetite (but such a high δ_{VJ} value is relatively independent of SIRM).

(5) We propose that the AF corresponding to the peak δ_{VJ} of the AF demagnetization spectra for MD magnetite grains is useful in estimating the average microcoercivity $<h_c>$.

Acknowledgements

This work was supported by the Bairen Program of the Chinese Academy of Sciences and NSFC grant 40221402. The studied natural magnetite samples were kindly provided by IKON Mining Company

References

Cui, Y., Verosub, K.L., Roberts, A.P., 1994, The effect of low-temperature oxidation on large multi-domain magnetite, *Geophys. Res. Lett.*, 21, 757-760.

Day, R., Fuller, M., Schmidt, V.A., 1977, Hysteresis properties of titanomagnetites: grain-size and compositional dependence, *Phys. Earth Planet. Inter.*, 13, 260-266.

Dunlop, D. J., 1987, Temperature dependence of magnetic hysteresis in 0.04-0.22 μm magnetites and implications for domain structure, *Phys. Earth Planet. Inter.*, 46, 100-119.

Dunlop, D.J., and Ö. Özdemir, *Rock magnetism: Fundamentals and Frontiers*, Cambridge University Press, New York, 1997.

Dunlop, D.J., Xu, S., Heider, F., 2004, Alternating field demagnetization, single-domain-like memory, and the Lowrie-Fuller test of multidomain magnetite grains (0.6–356 μm), *J. Geophys. Res.*, 109, B07102, doi:10.1029/2004JB003006.

Gilder, S., Le Goff, M., Chervin, J.C., Peyronneau, J., 2004, Magnetic properties of single and multi-domain magnetite under pressures from 0 to 6 GPa, *Geophys. Res. Lett.*, *31*, L10612, doi:10.1029/2004GL019844.

Gilder, S.A., Le Goff, M., Chervin, J.C., 2006, Static stress demagnetization of single and multidomain magnetite with implications for meteorite impacts, *High Pressure Research*, 26, 539-547, doi:10.1080/08957950601092085.

Hodych, J.P., 1982, Magnetostrictive control of coercive force in multidomain magnetite, *Nature*, 298, 542-544.

Hodych, J.P., 1990, Magnetic hysteresis as a function of low temperature in rocks: evidence for internal stress control of remanence in multi-domain and pseudo-single-domain magnetite, *Phys. Earth Planet. Inter.*, 64, 21-36.

Jackson, M., Worm, H., Banerjee, S.K., 1990, Fourier analysis of digital hysteresis data: rock magnetic applications, *Phys. Earth Planet. Inter.*, 65, 78-87.

Kakol, Z., Sabol, J., Sticker, J., Honig, J.M., 1992, Effects of low-level titanium(IV) doping on the resistivity of magnetite near the Verwey transition, *Phys. Rev., 46*, 1975-1978.

Kakol, Z., Sabol, J., Sticker, J., Kozkowski, A., Honig, J.M., 1994, Influence of titanium doping on the magnetocrystalline anisotropy of magnetite, *Phys. Rev.*, 49, 12767-12772.

Lowrie, W., Fuller, M., 1971, On the alternating field demagnetization characteristics of multidomain thermoremanent magnetization in magnetite, *J. Geophys. Res.*, 76, 6339-6349.

Muxworthy, A.R., Williams, W., 1999, Micromagnetic models of pseudo-single domain grains of magnetite near the Verwey transition, *J. Geophys. Res.*, 104, 29203-29218.

Muxworthy, A.R., McClelland, E., 2000a, Review of the low-temperature magnetic properties of magnetite from a rock magnetic perspective, *Geophys. J. Int.*, 140, 101-114.

Muxworthy, A.R., McClelland E., 2000b, The causes of low-temperature demagnetization of remanence in multidomain magnetite, *Geophys. J. Int.*, 140, 115-131.

Muxworthy, A.R., Dunlop, D.J., Özdemir, Ö., 2003, Low-temperature cycling of isothermal and anhysteretic remanence: microcoercivity and magnetic memory, *Earth Planet. Sci. Lett.,* 205, 173-184.

Nagata, T., Kobayashi, K., Fuller M., 1964, Identification of magnetite and hematite in rocks by magnetic observation at low temperature, *J. Geophys. Res.,* 69, 2111-2120.

Özdemir, Ö., 2000, Coercive force of single crystals of magnetite at low temperatures, *Geophys. J. Int.*, 141, 351-356.

Özdemir, Ö., Dunlop, D.J., 1995, Closure domains in magnetite, *J. Geophys. Res.*, 100, 2193-2209.

Özdemir, Ö., Dunlop, D.J., 1997, Effect of crystal defects and internal stress on the domain structure and magnetic properties of magnetite, *J. Geophys. Res.*, 102, 20,211-20,224.

Özdemir, Ö., Dunlop, D.J., 1999, Low-temperature properties of a single crystal of magnetite oriented along principal magnetic axes, *Earth Planet. Sci. Lett.*, 165, 229-239.

Özdemir, Ö., Dunlop, D.J., Moskowitz, B.M., 2002, Changes in remanence, coercivity and domain state at low temperatures in magnetite, *Earth Planet. Sci. Lett.*, 194, 343-358.

Ozima, M., Ozima, M., Nagata, T., 1964, Low temperature treatment as an effective means of "magnetic cleaning" of natural remanent magnetization, *J. Geomagn. Geoelectr.*, 16, 37-40.

Ozima, M., Ozima, M., Akimoto, S., 1964, Low temperature characteristics of remanent magnetization of magnetite, *J. Geomagn. Geoelectr.,* 16, 165-177.

Putnis, A., 1992, *Introduction to Mineral Sciences*, Cambridge University Press, Cambridge.

Roberts, A.P., Pike, C.R., Verosub, K.L., 2000, First-order reversal curve diagrams: a new tool for characterizing the magnetic properties of natural samples, *J. Geophys. Res.*, 105, 28,461-28,476.

Schabes, M.E., Bertram, H.N., 1988, Magnetization processes in ferromagnetic cubes, *J. Appl. Phys.,* 64, 1347-1357.

Sholpo, L.Y., Ivanov, V.A., Borisova, G.P., 1991, Thermomagnetic effects of reorganization of domain structure, *Izv., Phys. Solid Earth*, 27, 617-623.

Smirnov, A.V., Tarduno, J.A., 2002, Magnetic field control of the low-temperature magnetic properties of stoichiometric and cation-deficient magnetite, *Earth Planet. Sci. Lett.,* 194*,* 359-368.

Träuble, H., 1966, Magnetisierungskurve der Ferromagnetika II, in *Moderne Probleme der Metallphysik*, ed. Seeger, A., Springer Verlag, Berlin.

van Velzen, A.J., Dekkers, M.J., 1999. The incorporation of thermal methods in mineral magnetism of loess-paleosol sequences: a brief overview, *Chinese Sci. Bull.*, 44, (Supp. 1), 53-63.

van Velzen, A. J., Zijderveld, J.D.A., 1992, A method to study alterations of magnetic minerals during thermal demagnetization applied to a fine-grained marine marl (Trubi formation, Sicily), *Geophys. J. Int.*, 110, 79-90.

van Velzen, A.J., Zijderveld, J.D.A., 1995, Effects of weathering on single-domain magnetite in Early Pliocene marine marls, *Geophys. J. Int.*, 121, 267-278.

Weertman, J., 1978. Creep laws for the mantle of the earth, *Phil. Trans. R. Soc. London*, 288A, 9-22.

Williams, W., Dunlop, D.J., 1989, Three-dimensional micromagnetic modeling of ferromagnetic domain structure, *Nature,* 337, 634-637.

Xu, S., Merrill, R.T., 1989, Microstress and microcoercivity in multidomain grains, *J. Geophys. Res.*, 94, 10627-10636.

Xu, S., Merrill, R.T., 1992, Stress, grain size, and magnetic stability of magnetite, *J. Geophys. Res.*, 97, 4321-4329.

Xu, S., Dunlop, D.J., 1995, Toward a better understanding of the Lowrie-Fuller test, *J. Geophys. Res.*, 100, 22533-22542.

Yu, Y., Dunlop, D.J., Özdemir, Ö., 2002, Partial anhysteretic remanent magnetization in magnetite 1. Additivity, *J. Geophys. Res.*, 107, 2244, doi: 10.1029/2001JB001249.

Yu, Y., Dunlop, D.J., Özdemir, Ö., 2003a, On the resolution of multivectorial remanences, *Earth Planet. Sci. Lett.*, 208, 13-26.

Yu, Y., Dunlop, D.J., Özdemir, Ö., 2003b, Are ARM and TRM analogs? Thellier analysis of ARM and pseudo-Thellier analysis of TRM, *Earth Planet. Sci. Lett.*, 205, 325-336.

Yu, Y., Tauxe, L., Moskowitz, B.M., 2004, Temperature dependence of magnetic hysteresis, *Geochem. Geophys. Geosyst.*, 5, Q06H11, doi:10.1029/2003GC000685.

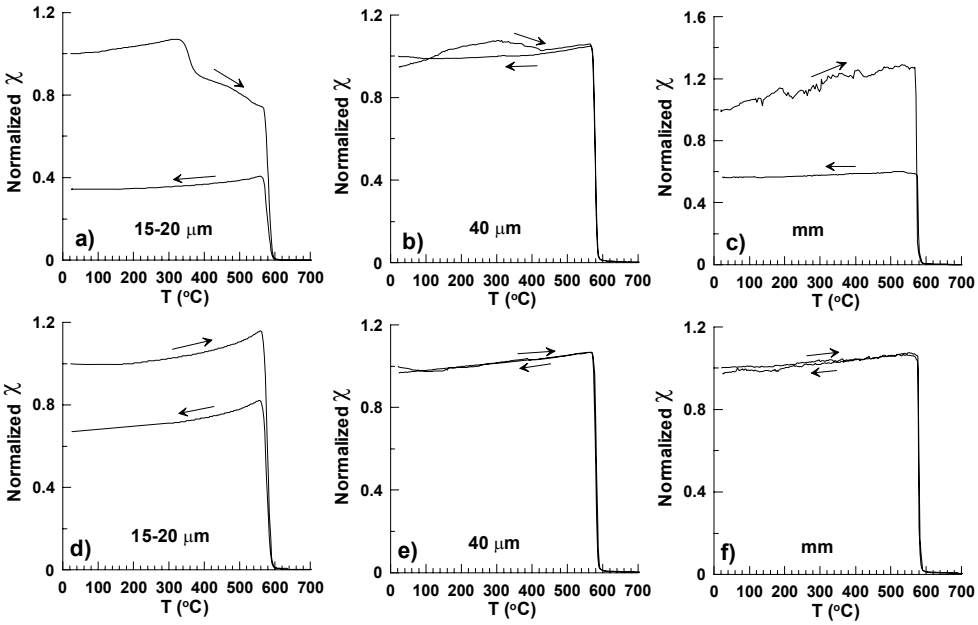

Fig. 1. Temperature dependence of magnetic susceptibility curves for (a, d) 15-20 μm, (b, e) 40 μm, and (c, f) mm-size magnetite grains. Arrows indicate heating and cooling cycles. (a-c) are first runs, and (d-f) are second runs.

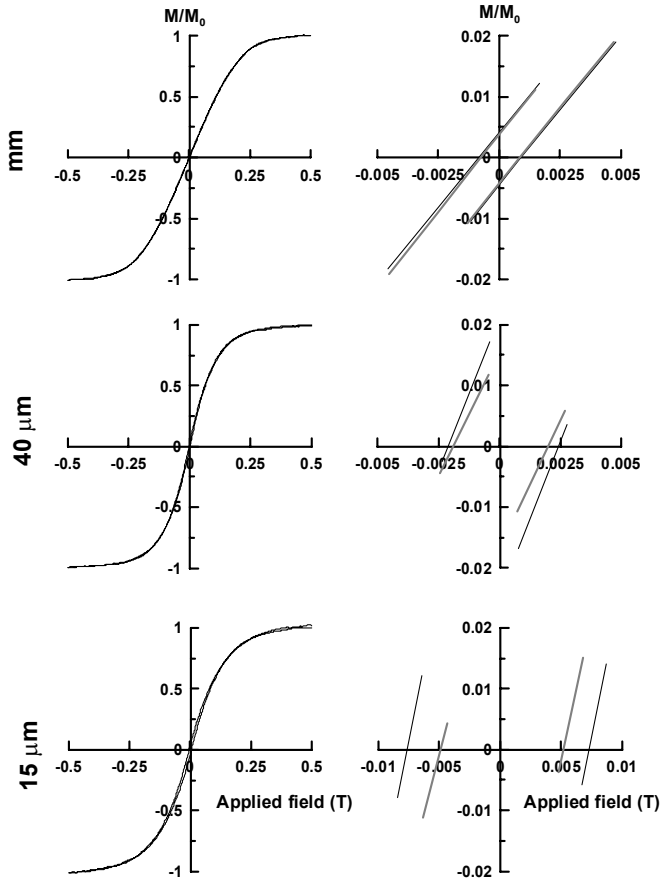

Fig. 2. Hysteresis loops for the raw and annealed magnetite samples. The left column is for the raw material. The right column compares the hysteresis behaviour for the unannealed ("raw"; black lines) and annealed (grey lines) samples.

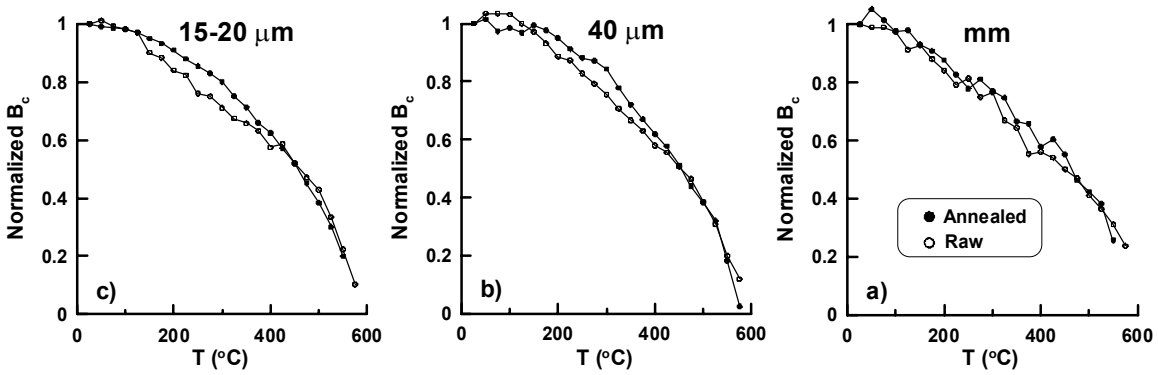

Fig. 3. Normalized temperature dependence of coercivity curves for (a) 15-20 μm, (b) 40 μm, and (c) mm-size magnetite grains. The open and solid circles indicate the unannealed ("raw") and annealed magnetite samples, respectively. The curves for "raw" samples lie below those for the annealed samples.

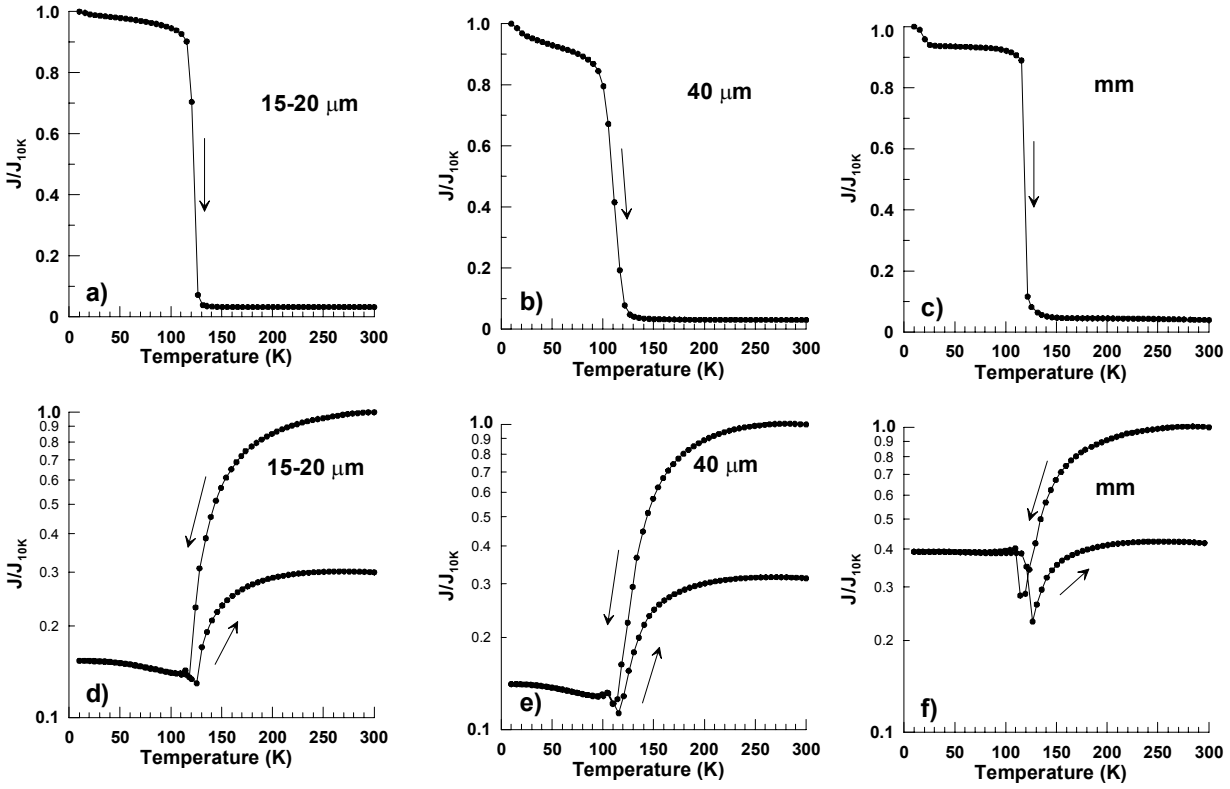

Fig. 4. LT-SIRM (above) and LTC (below) curves for (a, d) 15-20 μm, (b, e) 40 μm, and (c, f) mm-size magnetite grains. Arrows indicate heating and cooling cycles. Semi-logarithmic plots are used to enhance the weak pattern near the Verwey transition for the LTC curves (d-f).

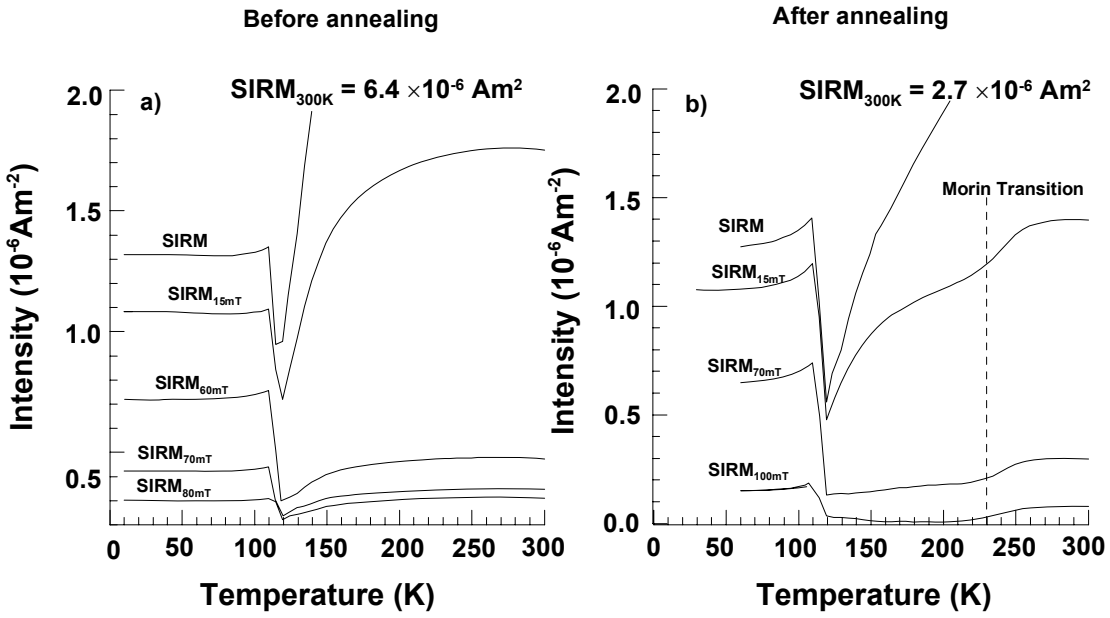

Fig. 5. Comparison of LTC of SIRM for the mm-size magnetite (a) before and (b) after annealing.

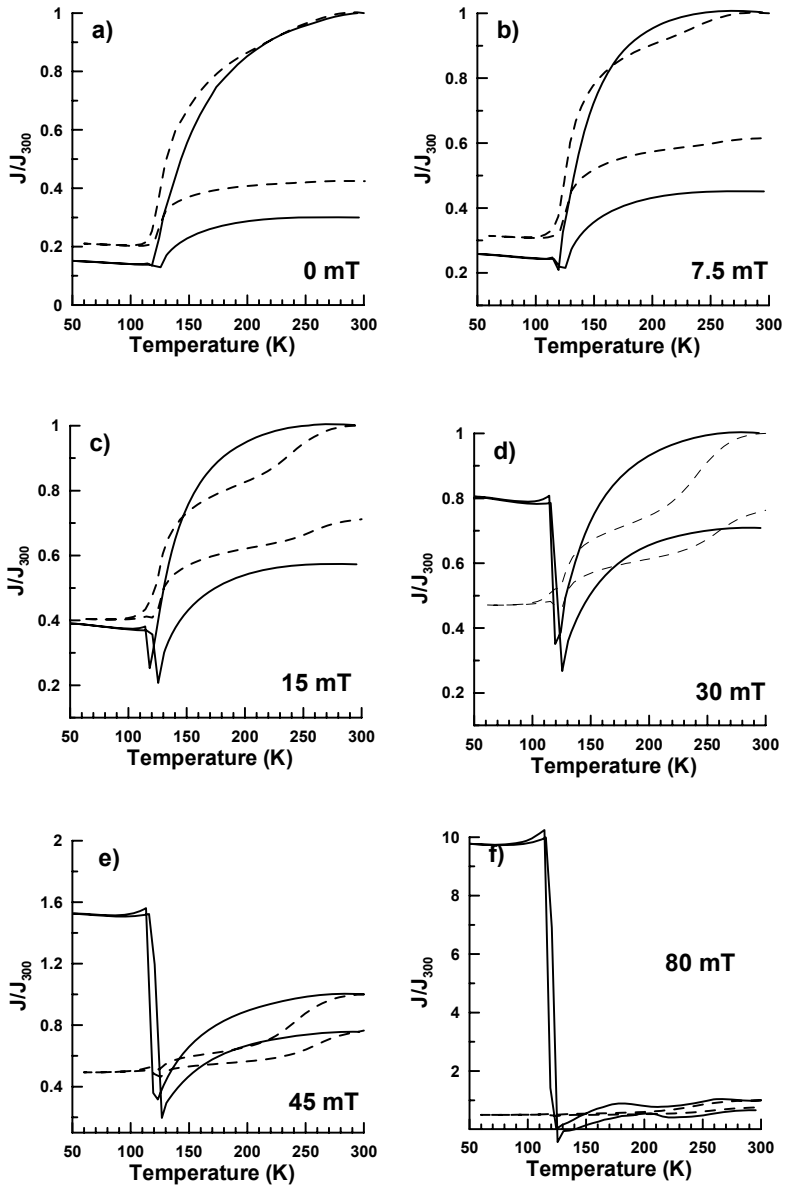

Fig. 6. LTC of normalized SIRMs for the 15-20 μm (dashed curves) and 40 μm (solid curves) magnetite grains after annealing. Numbers represent the peak alternating field.

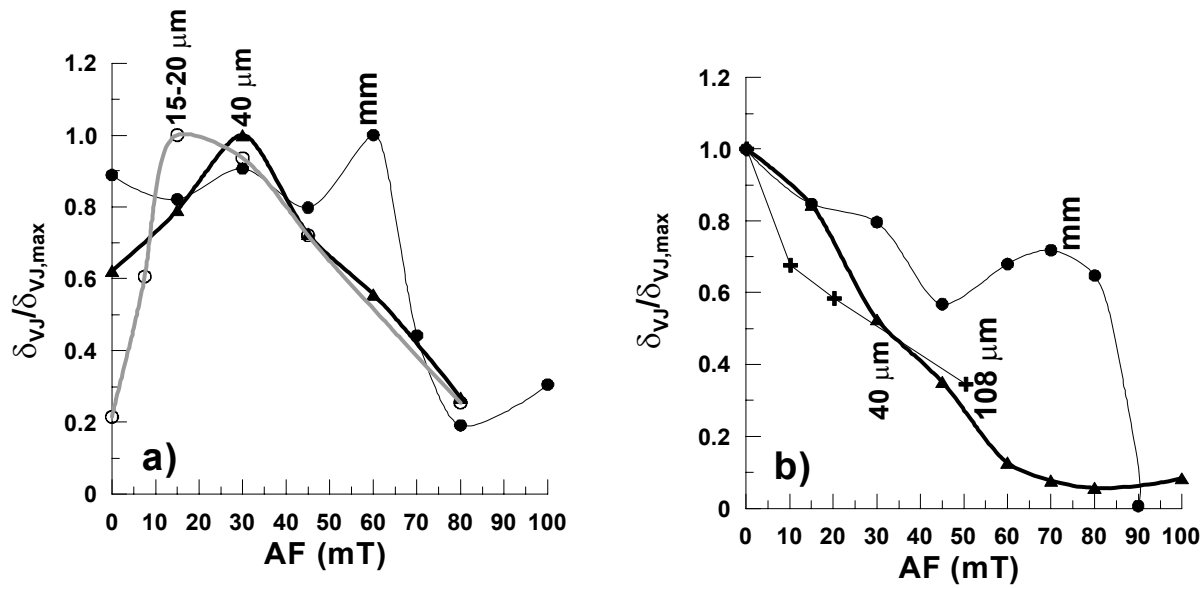

Fig. 7. AF demagnetization spectra of $\delta_{VJ}/\delta_{VJ,\,max}$ for the 15-20 μm, 40 μm and mm-size magnetite samples (a) before and (b) after annealing. No spectrum is shown for the 15-20 μm sample after annealing because δ_{VJ} was reduced so much by annealing that it could not be distinguished from the background remanence signals even after AF demagnetization at 30 mT. The AF demagnetization spectrum of δ_{VJ} for the stress-free MD magnetite (108 μm) from Muxworthy et al. (2003) is shown in (b) for comparison.

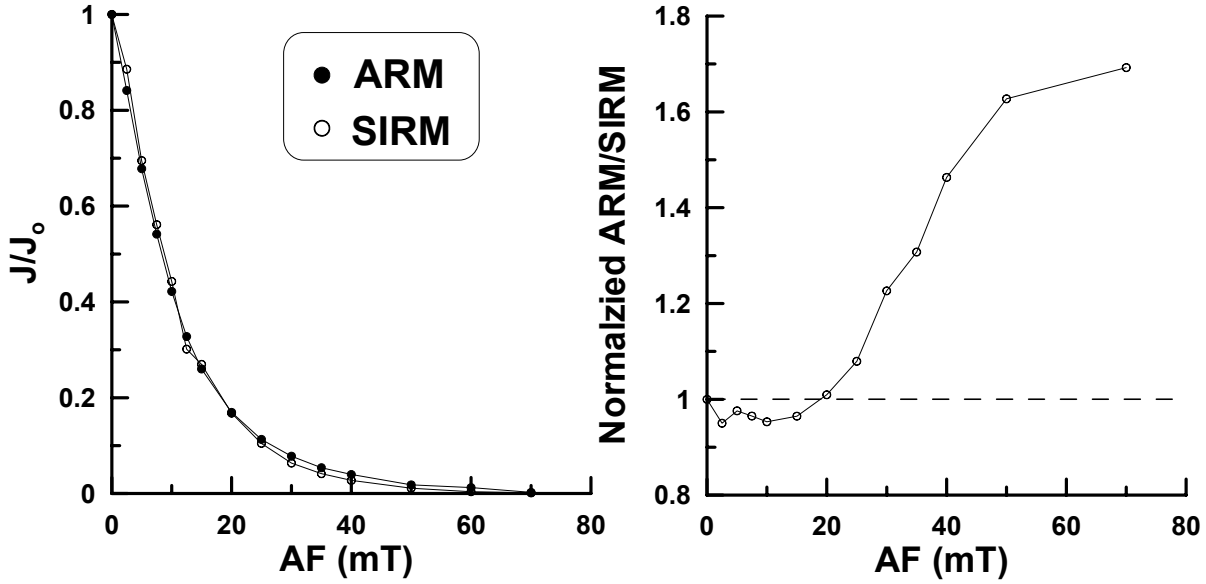

Fig. 8. AF demagnetization spectra of ARM and SIRM for the mm-size magnetite sample (a) before annealing, and (b) the normalized ARM/SIRM versus applied field.